Observation of self-accelerating Bessel-like optical beams along arbitrary trajectories

Juanying Zhao,[1,2,3] Peng Zhang,[2,4] Dongmei Deng,[2,5] Jingjiao Liu,[1] Yuanmei Gao,[2,6] Ioannis D. Chremmos,[7] Nikolaos K. Efremidis,[7] Demetrios N. Christodoulides,[3] and Zhigang Chen[2,8,*]

[1]*School of Optoelectronics, Beijing Institute of Technology, Beijing 100081, China*

[2]*Department of Physics and Astronomy, San Francisco State University, San Francisco, California 94132, USA*

[3]*CREOL/College of Optics, University of Central Florida, Orlando, Florida 32816, USA*

[4]*Currently with NSF Nanoscale Science and Engineering Center, University of California, Berkeley, California 94720, USA*

[5]*Laboratory of Nanophotonic Functional Materials and Devices, South China Normal University, Guangzhou 510631, China*

[6]*College of Physics and Electronics, Shandong Normal University, Jinan 250014, China*

[7]*Department of Applied Mathematics, University of Crete, Heraklion 71409, Greece*

[8]*TEDA Applied Physics School, Nankai University, Tianjin 300457, China*

Corresponding author: zhigang@sfsu.edu

We experimentally demonstrate self-accelerating Bessel-like optical beams propagating along arbitrary trajectories in free space. With computer-generated holography, such beams are designed to follow different controllable trajectories while their main lobe transverse profiles remain nearly invariant and symmetric. Examples include parabolic, snake-like, hyperbolic, hyperbolic secant, and even three-dimensional spiraling trajectories. The self-healing property of such beams is also demonstrated. This new class of optical beams can be considered as a hybrid between accelerating and nonaccelerating nondiffracting beams that may find a variety of applications.   © 2013 Optical Society of America

OCIS codes: 070.7345, 070.3185, 070.2580, 090.1760.

Over the past six years, self-accelerating Airy beams have stimulated substantial research interest [1–4]. Typically, such beams possess highly asymmetric transverse profiles, as originated from their ray structures that are associated with the curved caustics. Bessel beams, on the other hand, exhibit radially symmetric nondiffracting transverse profiles due to conical superposition of plane waves [5], and it was shown that their counterparts in the time domain can also self-accelerate along the longitudinal direction [6,7]. It has also been shown that Bessel beams can propagate along specific curved paths including spiraling trajectories [8–10]. Quite recently, we proposed that Bessel-like beams can be engineered to propagate along arbitrary trajectories in free space [11].

In this Letter, we report on the experimental demonstration of families of nondiffracting self-accelerating Bessel-like optical beams [11] that can follow parabolic, snake-like, hyperbolic, hyperbolic secant, and even three-dimensional (3D) spiraling trajectories. The main lobe of such beams remains invariant during propagation, and can even recover itself after being perturbed. The symmetric transverse beam profiles together with features of nondiffracting, self-healing, and trajectory tunability may be particularly attractive for various applications such as in optical trapping and manipulation [12,13].

Let us consider a self-accelerating Bessel-like beam propagating along a predesigned curved trajectory defined by $(f(z), g(z), z)$ in free space. According to the theory developed in [11], under the paraxial and slowly varying envelope approximations, the beam structure at input $z = 0$ is governed by

$$u(x, y) = \exp(-(x^2 + y^2)/w^2) \exp[iQ(x, y)], \quad (1)$$

where w is the characteristic beam size and $Q(x, y)$ is determined by the following equations:

$$Q(x, y) = \frac{k_0}{2} \int_0^z \{[f'(\zeta)]^2 + [g'(\zeta)]^2 - (\beta/k_0)^2\} d\zeta$$
$$- k_0 \frac{(f - x)^2 + (g - y)^2}{2z},$$
$$\beta^2 z^2/k_0^2 = [x - f(z) + zf'(z)]^2 + [y - g(z) + zg'(z)]^2, \quad (2)$$

where k_0 and β are the free-space and transverse wavenumbers, respectively. The underlying physical picture of such self-accelerating Bessel-like beams can be described as follows: an initial Gaussian beam is modulated by a specifically designed phase Q so that its constituent rays form a focal line along the desired trajectory $(f(z), g(z), z)$ in free space. These beams possess transverse field profiles close to the Bessel function $J_0(\beta r)$, and they "focus" at controllable distances while keeping remarkably invariant main lobes [11].

To experimentally demonstrate the self-accelerating Bessel-like beams, we utilize computer-generated holography via a spatial light modulator (SLM). Figure 1 depicts the schematic of our experimental setup, similar to those
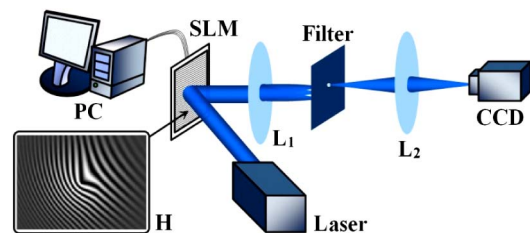

Fig. 1. (Color online) Experimental setup for generating self-accelerating Bessel-like beams via computer-generated holography. SLM, spatial light modulator; H, hologram; L, lens; CCD, charge-coupled device.

previously used for generating the autofocusing [13] and bottle-like beams [14]. A Gaussian beam emitted from an argon ion laser ($\lambda = 488$ nm) passes through the SLM programmed by a computer-generated hologram obtained by calculating the interference between the initial optical field $u(x, y)$ and a tilted plane wave. Upon reflection from the hologram, the encoded beam information is reconstructed via a typical $4f$ system with spatial filtering. A CCD camera is used to record the transverse patterns of the Bessel-like beam at different longitudinal positions. To map out the self-bending trajectory of the beam, a reference Gaussian beam reconstructed from a straight-line hologram in the SLM is used for calibrating the transverse beam position, instead of manually repositioning the CCD [15].

Figure 2 depicts the numerical and experimental results of a Bessel-like beam propagating along a parabolic trajectory $(f, g) = (z^2/2.6 \times 10^5, 0)$ produced with a computer-generated hologram shown in Fig. 2(a). [All the beam trajectories presented here, $(x, y) = (f(z), g(z))$ and z, are measured in millimeters and centimeters, respectively.] The designed beam profile encoded in the hologram represents a modulated Gaussian beam ($w = 30$), as directly calculated from Eqs. (1) and (2). Obviously, the reconstructed beam from the hologram indeed propagates along a parabolic trajectory as shown in Figs. 2(b) and 2(g). The transverse intensity patterns taken at different propagation distances clearly indicate the Bessel-like intensity distributions and the diffraction-resisting main lobes [see Figs. 2(c)–2(g), where the intensities are normalized], as expected from the initial beam design. Specifically, from Fig. 2, it can be seen that the beam accelerates along the designed parabolic path up to $z = 140$ cm and then it gradually loses the acceleration and the nondiffraction property due to the finite beam size

and the paraxial limitation. Importantly, the main lobe of the beam remains symmetric with unchanged beam-width during propagation, although the side lobes evolve from asymmetric profiles to symmetric Bessel profiles at about $z = 70$ cm, and then back to asymmetric profiles but with beam power shifted to the opposite side. Note that when the beam reaches its peak intensity in the center, its profile matches well with the Bessel function $J_0(\beta r)$. Measured beam sizes indicate that the main lobe does not diffract during entire propagation when compared to a Gaussian beam with the same size (not shown here). These experimental observations agree well with our theoretical prediction. We mention that, with the similar approaches developed in [15], the beam trajectory and the peak intensity position can be reconfigured and dynamically controlled with ease.

Next, following the similar aforementioned procedure, we demonstrate such Bessel-like beams with different designed trajectories. Our experimental results are juxtaposed in Fig. 3, where three examples at $g = 0$ are listed including a snake-like $f(z) = 0.03[1 - \cos(\pi z/350 - 0.2\pi)]$ [(a), (d)], a hyperbolic $f(z) = \sqrt{7.5 \times 10^{-7}z^2 - 2.6 \times 10^{-4}z + 0.05} - \sqrt{0.05}$ [(b), (e)], and a hyperbolic secant trajectory $f(z) = 0.06\,\mathrm{sech}[0.007(z - 315)]$ [(c), (f)]. Apparently, in all three cases, the observed trajectories agree well with the predesigned ones. Such curved trajectories clearly possess the ability to get over obstacles. Although overall the generated beams follow the predesigned trajectories, it can be seen from Figs. 3(d)–3(f) that the accelerating
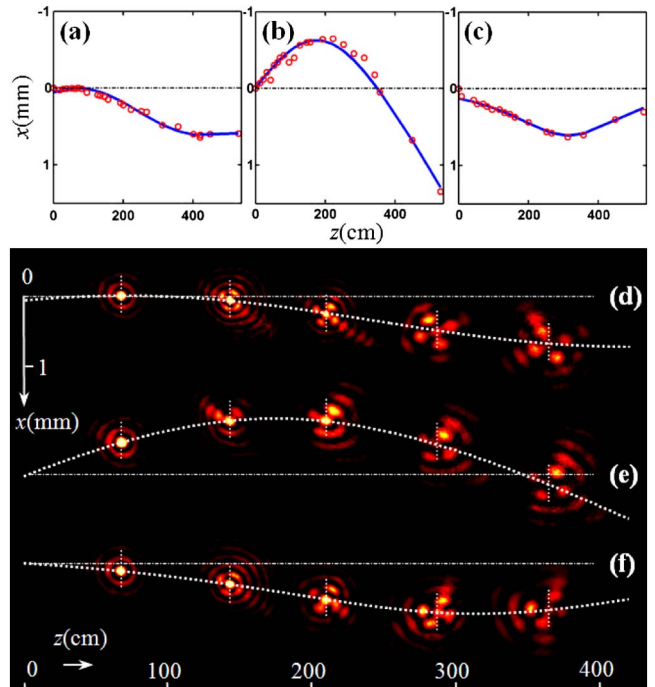
Fig. 3. (Color online) Experimental demonstration of self-accelerating Bessel-like beams along a snake-like [(a), (d)], a hyperbolic [(b), (e)], and a hyperbolic secant [(c), (f)] trajectory. In (a)–(c), the solid curves plot the predesigned trajectories and the circles represent experimental data. (d)–(f) Recorded transverse beam patterns at different positions marked in the predesigned trajectories (dashed curve) corresponding to (a)–(c), respectively.
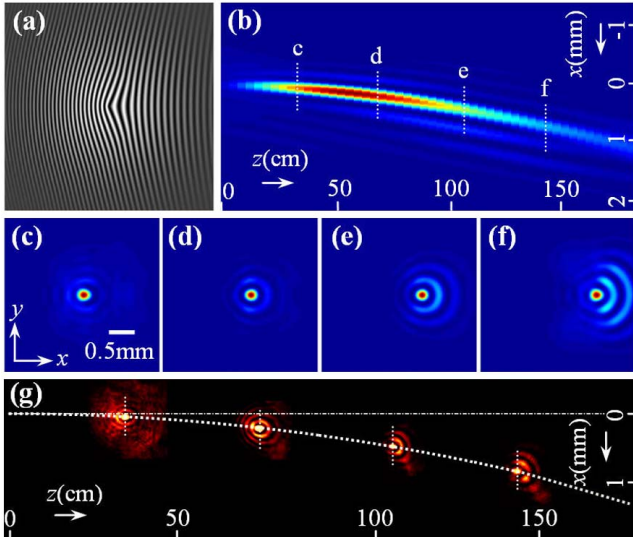
Fig. 2. (Color online) Numerical and experimental demonstrations of a self-accelerating Bessel-like beam along a parabolic trajectory. (a) Computer-generated hologram; (b) numerically simulated side-view propagation of the generated beam; (c)–(f) snapshots of the transverse intensity patterns taken at the planes marked by the dashed lines in (b); and (g) experimentally recorded transverse beam patterns at different positions marked in the predesigned parabolic trajectory (dashed curve) corresponding to (b).
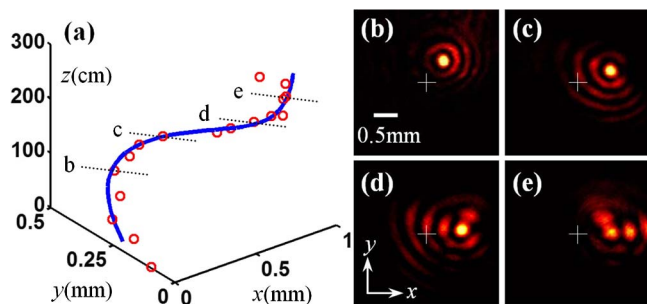
Fig. 4.   (Color online) Experimental demonstration of self-accelerating Bessel-like beams along a 3D curved trajectory. (a) Measured (circles) versus the predesigned (solid curve) beam trajectory; (b)–(e) transverse beam patterns at different marked positions in (a), where the cross marks the center of the reference Gaussian beam.
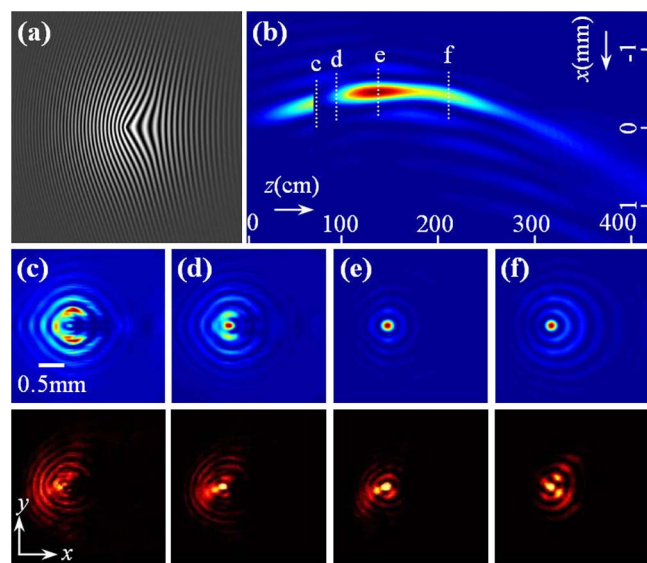

Fig. 5.   (Color online) Numerical and experimental results of the self-healing property of a Bessel-like beam along a hyperbolic trajectory. (a) Hologram and (b) numerical simulation of the side-view propagation of the generated beam, when its main lobe is partially blocked by an opaque wire. (c)–(f) Display the transverse intensity snapshots from the simulation (top) and experiment (bottom) at different planes marked in (b).

beam tends to break up into pieces and lose its Bessel-like transverse structure, possibly due to the use of limited aperture size and symmetry breaking, for example, due to the filtering process in the current experiment.

Furthermore, we demonstrate that self-accelerating Bessel-like beams can follow 3D trajectories. A typical example for $x = f(z) = 0.4 \tanh[0.02(z - 70)] + 0.04$ and $g(z) = 0.046 \operatorname{sech}[0.02(z - 70)]$ is shown in Fig. 4. Again, the measured trajectory matches well with the predesigned one. Recorded transverse beam patterns indicate clearly that the beam bends in both x and y directions, while its main lobe remains nearly symmetric and diffraction-free.

Finally, we show the self-healing property of such self-accelerating Bessel-like beams. As an example, numerical and experimental results of a hyperbolic accelerating beam are shown in Fig. 5 when the beam is partially blocked by an opaque wire with a diameter of 0.2 mm at $z = 70$ cm. Apparently, right after the wire, the main lobe and part of the rings of the beam are

blocked as shown in Fig. 5(c). Figures 5(b)–5(f) clearly indicate that the beam can restore its beam structure during subsequent propagation, as expected from the theory [11]. In addition, we have also observed the self-healing ability of the beams shown in Figs. 3 and 4.

In summary, we have experimentally demonstrated self-accelerating Bessel-like beams propagating along arbitrary trajectories and their self-healing properties. Such beams gifted with nondiffracting symmetric main lobes may find a variety of applications, including, for example, particle manipulation [12,13]. Moreover, our method might be readily extended to beyond the paraxial limit [16–20].

References

1. G. A. Siviloglou and D. N. Christodoulides, Opt. Lett. **32**, 979 (2007).
2. G. A. Siviloglou, J. Broky, A. Dogariu, and D. N. Christodoulides, Phys. Rev. Lett. **99**, 213901 (2007).
3. E. Greenfield, M. Segev, W. Walasik, and O. Raz, Phys. Rev. Lett. **106**, 213902 (2011).
4. Y. Hu, G. A. Siviloglou, P. Zhang, D. N. Christodoulides, and Z. Chen, in *Nonlinear Photonics and Novel Phenomena*, Z. Chen and R. Morandotti, eds. (Springer, 2012).
5. J. Durnin, J. J. Miceli, Jr., and J. H. Eberly, Phys. Rev. Lett. **58**, 1499 (1987).
6. M. Clerici, D. Faccio, A. Lotti, E. Rubino, O. Jedrkiewicz, J. Biegert, and P. Di Trapani, Opt. Express **16** 19807 (2008).
7. H. Valtna-Lukner, P. Bowlan, M. Lõhmus, P. Piksarv, R. Trebino, and P. Saari, Opt. Express **17**, 14948 (2009).
8. J. Morris, T. Cizmar, H. Dalgarno, R. Marchington, F. Gunn-Moore, and K. Dholakia, J. Opt. **12**, 124002 (2010).
9. V. Jarutis, A. Matijošius, P. D. Trapani, and A. Piskarskas, Opt. Lett. **34**, 2129 (2009).
10. A. Matijošius, V. Jarutis, and A. Piskarskas, Opt. Express **18**, 8767 (2010).
11. I. D. Chremmos, Z. Chen, D. N. Christodoulides, and N. K. Efremidis, Opt. Lett. **37**, 5003 (2012).
12. J. Baumgartl, M. Mazilu, and K. Dholakia, Nat. Photonics **2**, 675 (2008).
13. P. Zhang, J. Prakash, Z. Zhang, M. S. Mills, N. K. Efremidis, D. N. Christodoulides, and Z. Chen, Opt. Lett. **36**, 2883 (2011).
14. P. Zhang, Z. Zhang, J. Prakash, S. Huang, D. Hernandez, M. Salazar, D. N. Christodoulides, and Z. Chen, Opt. Lett. **36**, 1491 (2011).
15. Y. Hu, P. Zhang, C. Lou, S. Huang, J. Xu, and Z. Chen, Opt. Lett. **35**, 2260 (2010).
16. I. Dolev, R. Bekenstein, J. Nemirovsky, and M. Segev, Phys. Rev. Lett. **108**, 163901 (2012).
17. P. Zhang, Y. Hu, D. Cannan, A. Salandrino, T. Li, R. Morandotti, X. Zhang, and Z. Chen, Opt. Lett. **37**, 2820 (2012).
18. F. Courvoisier, A. Mathis, L. Froehly, R. Giust, L. Furfaro, P. A. Lacourt, M. Jacquot, and J. M. Dudley, Opt. Lett. **37**, 1736 (2012).
19. P. Zhang, Y. Hu, T. Li, D. Cannan, X. Yin, R. Morandotti, Z. Chen, and X. Zhang, Phys. Rev. Lett. **109**, 193901 (2012).
20. P. Aleahmad, M.-A. Miri, M. S. Mills, I. Kaminer, M. Segev, and D. N. Christodoulides, Phys. Rev. Lett. **109**, 203902 (2012).